PROCEEDINGS B

royalsocietypublishing.org/rspb

Research

Cite this article: He S, Deng Y, Zhang Y, Stuart-Fox D, Liu Y, Ma L. 2026 From colour to heat: linking visible and near-infrared reflectance in birds. *Proc. R. Soc. B* **293**: 20253333.
https://doi.org/10.1098/rspb.2025.3333

Received: 29 December 2025
Accepted: 4 June 2026

Subject Category:
Ecology

Subject Areas:
ecology, physiology , evolution

Keywords:
plumage, infrared, thermoregulation, heat balance, radiation, reflectance

Authors for correspondence:
Yang Liu
e-mail: liuy353@mail.sysu.edu.cn
Liang Ma
e-mail: maliang26@mail.sysu.edu.cn

Electronic supplementary material is available online at https://doi.org/10.6084/m9.figshare.c.8536173.

THE ROYAL SOCIETY PUBLISHING

From colour to heat: linking visible and near-infrared reflectance in birds

Siqi He[1], Yilin Deng[1], Yucheng Zhang[1], Devi Stuart-Fox[2], Yang Liu[1] and Liang Ma[1]

[1]School of Ecology, Sun Yat-Sen University, Shenzhen, Guangdong, People's Republic of China
[2]School of Biosciences, The University of Melbourne, Melbourne, Victoria, Australia

SH, 0009-0000-8029-021X; DS-F, 0000-0003-3362-1412; YL, 0000-0003-4580-5518

Feather reflectance in visible (VIS) and near-infrared (NIR) wavelengths influences avian heat balance by modulating the absorption of solar energy, yet the evolutionary and ecological patterns of NIR reflectance remain poorly understood. We developed a cross-taxonomic predictive framework linking NIR to VIS reflectance using a full-spectrum dataset of 531 bird species from 23 orders and 106 families, integrating 439 newly measured spectra with published data. Across species, VIS and NIR reflectance were strongly correlated (R^2 = 0.667), but regression slopes differed significantly among orders, indicating lineage-specific spectral scaling. When controlling for visible coloration, NIR reflectance still varied markedly across orders, revealing taxon-specific thermal properties beyond colour. Morphological and ecological traits further predicted these patterns, with hand-wing-index, migratory status, habitat types, habitat temperature and precipitation all exerting significant effects on NIR reflectance. Residual analysis revealed that Gruiformes, Pelecaniformes and Charadriiformes (i.e. waders, gulls, terns and allies) showed low and variable NIR reflectance, possibly reflecting structural adaptations to heterogeneous thermal environments. Collectively, our results provide the first large-scale, phylogenetically informed framework for predicting NIR reflectance from VIS data, advancing mechanistic understanding of avian thermal adaptations.

1. Introduction

Plumage reflectance plays a critical role in mediating how birds interact with solar radiation, influencing their thermal and water balance [1–3]. This function is particularly important in open environments where birds are directly exposed to sunlight [4–7]. Differences in reflectance can therefore shape how species respond to thermal stress, affecting their physiology, their behaviour and potentially their fitness. Understanding interspecific variation in plumage reflectance is thus key to predicting how birds cope with rising temperatures and more frequent heat extremes under climate change [5,6].

Existing measurements of avian plumage reflectance exhibit a strong bias, with most data concentrated in the visible (VIS) spectrum (300–700 nm) [8,9], while near-infrared (NIR) reflectance (700–2500 nm) has received much less attention. However, NIR wavelengths account for approximately 55% of absorbed solar energy [10], meaning that variation in NIR reflectance can strongly influence the amount of solar radiation converted into heat and thereby affect an individual's heat balance [5,10,11]. From a physical perspective, NIR reflectance in feathers is primarily determined by micro-structural properties rather than pigment absorption, generating substantial variation in reflectance that is often decoupled from visible coloration [10,12]. From an evolutionary perspective, because NIR wavelengths are not perceived by most organisms, variation in NIR reflectance is more likely to

be shaped by selection related to thermoregulation rather than signalling, potentially leading to distinct evolutionary trajectories across environments [10,13]. The limited availability of NIR reflectance data reflects both the historical focus on visible coloration in studies of signalling, camouflage and sexual selection [11,13,14] and the high cost and limited accessibility of full-spectrum spectrometry. However, over the past decade, NIR reflectance has been increasingly recognized as essential for modelling avian heat balance and physiological performance [5,12,15]. Recent advances in biophysical modelling have demonstrated that incorporating full-spectrum reflectance data can substantially improve predictions of avian physiological responses to climate change, including body temperature, metabolic rate, and evaporative water loss [5–7]. However, the current paucity of NIR data continues to constrain the taxonomic and geographic applicability of such models, compelling many studies to presume uniform reflectance values across species [15,16], and thereby reducing the ecological relevance and precision of model outputs.

In other domains of trait-based ecology, when key data are missing, predictive models based on correlated traits have been used successfully to fill gaps, such as using body length to infer body mass [17–19]. An analogous approach for reflectance would allow researchers to estimate NIR values from the more commonly available VIS data, thereby reducing costs and expanding the applicability of reflectance-based analyses. Existing studies have shown a strong correlation between VIS and NIR reflectance, often well described by simple linear relationships [5,12]. This coupling arises because they are both part of a continuous spectrum that changes gradually, and they share an underlying feather microstructure [12,20,21]. Nonetheless, reflectance profiles and associated VIS-NIR relationships can vary substantially due to the diversity of underlying pigments and structures. Additionally, while VIS reflectance may be influenced by both pigments and structures, NIR reflectance is largely structure-driven because most pigments have absorbance peaks confined largely to the visible spectrum [10,13,22]. Thus, VIS and NIR reflectance are expected to covary, but the strength and slope of this relationship are not strongly mechanistically constrained.

Variation in the relationship between VIS and NIR reflectance may arise when selective pressures act differently on the two spectral regions. For instance, thermoregulatory selection can modify solar reflectivity in the NIR without substantially altering visible coloration, which is expected to be under selection for anti-predator or signalling functions [10]. In such cases, ecological or thermal pressures may produce clade-specific differences in the NIR–VIS relationship, leading to variation in slopes or residual reflectance among taxa. Despite these insights, existing studies remain limited in both sample size and taxonomic breadth. For example, Stuart-Fox *et al.* [12] analysed approximately 50 species from 12 avian orders, mainly Passeriformes, Charadriiformes and Anseriformes, while Medina *et al.* [5] examined around 90 Australian species from 14 orders, most of which belonged to Passeriformes. Importantly, these studies focused on estimating a single, global VIS–NIR relationship and did not explicitly test how this relationship varies among clades. As a result, it remains unclear whether the VIS–NIR relationship is consistent across the avian tree of life or varies with morphometric and ecological traits such as hand-wing index (HWI), habitat type or environmental conditions.

In this study, we ask the following two key questions. (i) Does a generalizable relationship between VIS and NIR reflectance exist across birds? (ii) To what extent does this relationship vary among clades and in association with morphological and ecological traits? We hypothesize that, while VIS and NIR reflectance are positively correlated due to shared structural constraints, the strength and slope of this relationship will vary among clades, reflecting lineage-specific selective pressures on thermal properties and trade-offs with competing selection pressures. To address these questions, we assembled a comprehensive dataset by combining direct spectrometer measurements from 439 species with literature-derived data, yielding reflectance records for 531 species across 106 families and 23 avian orders. We quantified relationships between VIS and NIR reflectance within and between clades and developed predictive linear models. By generating order-specific regression equations, we provide a practical framework for estimating NIR reflectance in taxa that lack direct measurements. In addition, we investigated inter-clade differences in NIR reflectance by analysing regression slopes and residuals, and identified factors influencing variation. This dataset not only expands the empirical basis for avian thermal ecology but also enables broader application of mechanistic models to assess species' physiological responses to climate change.

To examine how morphological and ecological traits might influence the VIS–NIR reflectance relationship, we incorporated eight candidate predictors into our models: temperature, precipitation, habitat type, habitat density, body mass, wing length, HWI, and migratory status. These variables were selected based on prior evidence linking them to plumage coloration or thermoregulatory adaptation in birds [9,11,12,22–24]. Environmental factors such as climate and habitat structure have been shown to affect plumage coloration through selection for camouflage and thermal balance [11,22], while morphological traits like body size and feather length can modulate reflectance via structural or aerodynamic constraints [9,12]. Migration-related traits, including HWI and migratory strategy, may also shape plumage reflectance patterns due to the thermal and aerodynamic demands of long-distance flight [23,24].

2. Methods

(a) Specimen selection

We measured plumage reflectance from 350 to 1700 nm (VIS and NIR) for 1980 individuals representing 439 species, 89 families, and 22 orders, with the NIR range (700–1700 nm) selected because it captures approximately 88% of the total solar irradiance available in the 700–2500 nm spectrum, a finding derived from numerical integration of the ASTM G173-03 standard terrestrial solar spectral irradiance. All specimens were from the Museum of Biology, Sun Yat-Sen University (SYSBM) and National Animal Collection Resource Center, Institute of Zoology, Chinese Academy of Sciences (NACRC, IOZCAS). Data

on the specimens obtained from NACRC, IOZCAS are publicly available [25,26], while those from SYSBM are provided in the electronic supplementary material. When available, we used six adult specimens (three males and three females) for measurements and recorded the order, family, sex and identification number of the specimen. If the species had both breeding and non-breeding plumage forms, specimens in breeding plumage were preferred as measurement specimens. If there were fewer than six specimens in breeding plumage, we measured the remaining specimens in non-breeding plumage.

(b) Spectral measurements and processing

Measurements were made using the DCS-3517 dual-channel wide-range spectrum analyser, which consists of two spectrometers (USB2000+ [350–1000 nm] and NIRQuest [900–1700 nm]) equipped with an ISP-REF integrating sphere with halogen light source (350–2500 nm wavelength range; Ocean Optics, Florida). The dual-spectrometer configuration allows simultaneous acquisition of VIS and NIR signals, improving sensitivity and signal-to-noise ratio across the full spectral range compared to single-detector systems. The integrating sphere provides uniform, highly diffuse illumination via a Spectralon-coated interior (>98% reflectance in the VIS–NIR range), enabling hemispherical reflectance measurements that are independent of illumination and viewing geometry. This configuration minimizes measurement error associated with angle-dependent reflectance, which is a common limitation of fibre-optic probe-based approaches, and thus provides a more robust estimate of reflectance for non-planar surface (bird plumage) [27]. Reflected light was directed to the two spectrometer channels through a Y-split fibre. Measurements were calibrated relative to a diffuse reflection standard (PTFE Standard whiteboard: 97–99% reflectance across the spectral range of 350–1700 nm; Biaoqi Optics).

To prevent specimen damage and to avoid contamination of the integrating sphere, the sampling port (a circular aperture with a diameter of 0.5 cm) was covered with a 1-mm-thick quartz glass plate (JGS1; transmissivity >97% across the VIS-NIR range [28]). To account for potential measurement bias introduced by the quartz glass, we conducted calibration experiments by measuring the same specimens (and identical regions) with and without the glass plate. Based on these paired measurements, we derived linear correction models (see electronic supplementary material, section S1), which were applied to all reflectance data collected with the glass in place. Because the correction models do not fully explain all variation, we further conducted a sensitivity analysis to evaluate how uncertainty in the correction parameters (α and b) might affect downstream results. Specifically, we recalculated order-specific regression parameters using the 2.5% and 97.5% quantiles of the correction coefficients across 1000 phylogenetic trees (see electronic supplementary material, section S1). This analysis showed that the reported slopes and intercepts of the order-specific VIS–NIR relationships are robust to uncertainty in the correction procedure.

Reflectance was measured across VIS (350–700 nm) and NIR (700–1700 nm) wavelengths at six distinct regions on each specimen: the nape, mantle, rump, breast, belly and wing (figure 1). Each region was measured twice, and the results were averaged to represent each species. For areas with multiple colours, we measured the dominant colour, which was the one with the highest area percentage for that body region. When body regions had fine patterning or comprised colours with similar areas, we selected the junctions between colours to provide an average measure.

(c) Literature survey for reflectance data

Besides measuring plumage reflectance from museum specimens, we also compiled plumage reflectance data in the VIS and NIR ranges from the literature. We conducted a literature search using Web of Science, Google Scholar and ResearchGate, and generated search terms by combining the keywords 'near infrared' (same as 'near-infrared'), 'colour', 'visible light', 'radiation', 'reflectance', 'birds' and 'avian'. We screened articles returned by the search and retained those that reported specimen-based reflectance measurements spanning both the VIS and NIR spectra. Detailed information for all literature sources, including species numbers, spectral ranges, and data provenance, is provided in electronic supplementary material, table S3. To maximize comparability across studies, we used the original spectral reflectance data, either from publicly available datasets or by obtaining the raw spectra directly from authors when these were not published. Rather than relying on summary values reported in the original studies, we recalculated arithmetic mean reflectance from the raw spectra for each sample. We defined VIS reflectance as the arithmetic mean reflectance across 300–700 nm. NIR reflectance was calculated from 700 nm to the maximum available wavelength reported in each study, up to 2500 nm when available. Although the exact upper wavelength limits differed among studies because of instrumentation constraints, such variation is common in reflectance research and often reflects unavoidable differences in measurement setup [5,15,29]. To preserve as much information as possible from the original datasets, we used the full wavelength range available in each study, rather than cutting all datasets to the same narrower range. Using this approach, we extracted reflectance data for 1170 individuals of 95 species belonging to 39 families and 15 orders of birds. Among these, three species were also measured directly by us. Combining reflectance data collected from our own measurements and the literature, we generated a dataset of full-spectrum reflectance of bird plumage for 531 species, 106 families and 23 orders.

(d) Phylogenetic tree construction

To account for phylogenetic non-independence, we used phylogenetic trees from http://birdtree.org [30]. We downloaded 1000 random trees using the 'Hackett backbone'. To facilitate downstream phylogenetic analyses, we constructed a species-level tree for the combined dataset using the 'ggtree' R package [31]. For tree selection, we used the 'phangorn' R package [32] to generate maximum clade credibility (MCC) trees, and finally constructed a consensus phylogenetic tree covering the target bird species.

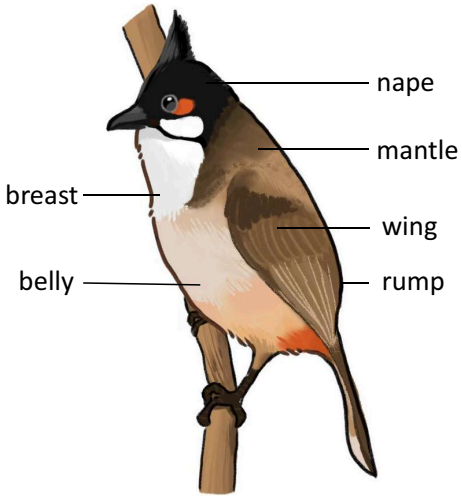

Figure 1. Illustration of plumage areas measured for each specimen. Measurements of the wing area are mainly concentrated on the coverts of the specimen, and measurements of some small species also cover the flight feathers.

(e) Statistical analyses

Prior to statistical analyses, we log-transformed all VIS and NIR data to better meet the assumptions of linear modelling. And the slopes can be interpreted as describing the allometric relationship between VIS and NIR reflectance. In all clades, slopes were below 1, indicating hypoallometric relationships, with NIR reflectance increasing less than proportionally relative to VIS reflectance. Nevertheless, variation in slope among clades still reflects differences in the strength of VIS–NIR coupling. In sexually dimorphic species, males and females showed significant differences in mean NIR and VIS reflectance. However, by fitting a linear model including the interaction between VIS and sex, we found that sex did not significantly affect the slope of the NIR–VIS relationship (electronic supplementary material, figure S2). Therefore, we pooled all individuals—males, females and unsexed individuals—for subsequent analyses. It is important to note that when applying our equation to predict NIR reflectance for sexually dimorphic species, the VIS data used for prediction should correspond to the same sex (i.e. NIR values predicted from male VIS data should be interpreted as male-specific estimates), in order to control for mean-level differences between sexes. We first fitted a simple ordinary least-squares (OLS) linear model to confirm the strong correlation between NIR and VIS reflectance for all species ($R^2 = 0.667$). This model was used only as a descriptive summary of the overall VIS-NIR relationship, rather than for the main inferential analyses. Although the model residuals did not pass the Shapiro–Wilk test ($W = 0.861$, $p < 0.001$), the histograms showed a symmetrical distribution and no extreme outliers. The Breusch–Pagan test indicated no significant heteroscedasticity ($BP = 1.395$, $p = 0.238$). Given the large sample size ($n = 531$), slight deviations from normality were unlikely to substantially affect the overall descriptive pattern of the relationship [33].

Next, we controlled for phylogenetic non-independence using the R package 'caper' and constructed a phylogenetic generalized least squares (PGLS) linear model for all species. For each order, we fitted a PGLS model on each posterior tree (λ estimated by ML per fit), retaining the slope and intercept estimates. We summarized phylogenetic uncertainty in topology by reporting the median estimate and a 95% equal-tailed credible interval (2.5th–97.5th percentiles) across up to 1000 trees. These intervals reflect across-tree variation (phylogenetic uncertainty) rather than within-tree standard errors. To test whether the relationship between NIR and VIS reflectance differed across taxa, we used PGLS models implemented in the 'nlme' package and analyses were based on a pruned MCC tree. To ensure sufficient sample sizes for order-level comparisons, we retained only those orders represented by at least six species. We modelled NIR reflectance as a function of VIS reflectance, order, and their interaction using restricted maximum likelihood (REML) estimation. To compare the level of variation in NIR reflectance among orders, we extracted and compared the residuals and slopes among lineages.

We obtained data on annual mean precipitation and annual mean temperature over the distribution range from Delhey *et al.* [24], and data on wing length, mass, habitat types, habitat density, migration type and HWI from Tobias *et al.* [34]. To evaluate how morphological and ecological traits were associated with NIR reflectance after accounting for VIS reflectance and phylogenetic relatedness, we fitted PGLS models with Pagel's λ estimated by maximum likelihood across 1000 phylogenetic trees. For each tree, we performed an exhaustive search of all possible subsets of candidate predictors, while always retaining VIS reflectance in the model. The best-supported model for each tree was identified using corrected Akaike Information Criterion (AICc), and only models that improved on the null model by more than 3 AICc units ($\Delta AICc > 3$) were considered supported [35]. The most frequently selected best model across trees was subsequently re-fitted under REML for each of the 1000 trees to obtain the distribution of regression coefficients. Support probabilities for individual predictors were quantified as their frequency of inclusion in the best-supported models across trees. For each predictor in this model, we extracted slope, intercept, t-value and the p-value across 1000 trees. We report the results of the best models in electronic supplementary information. All statistical analyses were performed using R 4.4.3 [36].

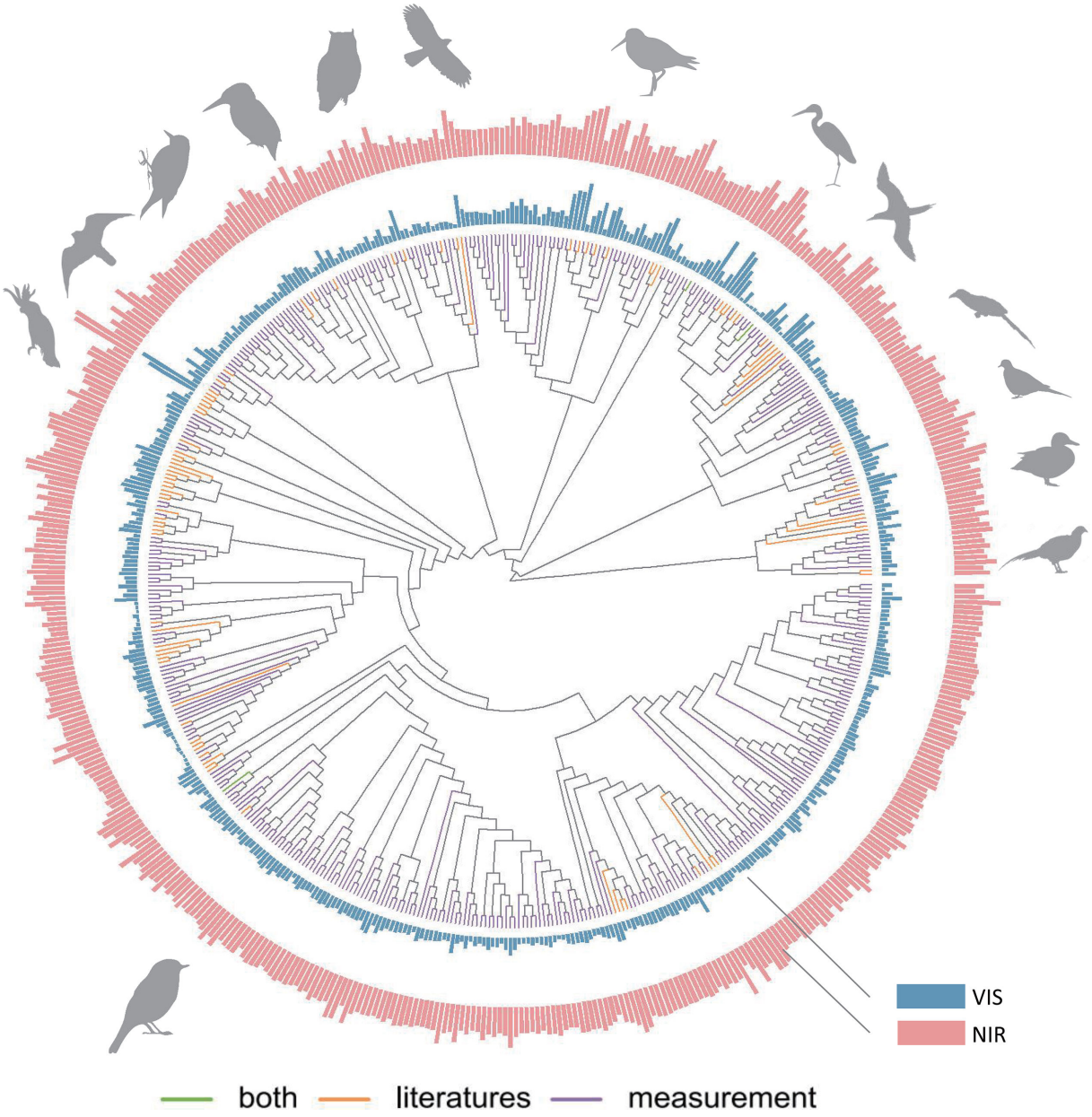

Figure 2. VIS and NIR plumage reflectance of 531 bird species in the dataset. Phylogenetic distribution of mean VIS (blue bars) and NIR (red bars) plumage reflectance of 531 bird species in the dataset. Branches colours indicate data sources: direct measurements (purple), literature-based data (orange), or both (green). Phylogenetic relationships are based on the Hackett backbone from birdtree.org.

3. Results

(a) Data coverage

Our dataset comprises full-spectrum (300–1700 nm) reflectance data for 531 avian species, representing 5.25% of described bird species. Of these, 439 species were measured directly using museum specimens, while reflectance data for an additional 110 species were compiled from the literature. Three species were represented in both sources (figure 2).

(b) Variation in VIS and NIR reflectance across bird orders

Across the 23 bird orders included in our dataset, both VIS and NIR reflectance exhibited substantial among-order variation ($p < 0.05$). The distribution of NIR reflectance showed a clear gradient, with several orders (e.g. Suliformes, Caprimulgiformes) displaying consistently lower NIR reflectance, whereas others (e.g. Anseriformes, Columbiformes) exhibited higher values. VIS reflectance broadly followed the same ordering pattern. Some orders maintained similar reflectance profiles across both spectral domains, whereas others showed divergent VIS–NIR patterns, suggesting order-specific spectral properties potentially linked to habitat use, ecological niche or plumage microstructure (figure 3). In certain sexually dimorphic species, differences in VIS and NIR reflectance are also observed between males and females. However, sex did not influence the relationship between these two reflectance values which meant the patterns of reflectance variation are similar across both sexes. Consequently, we did not incorporate the sex factor into our equations.

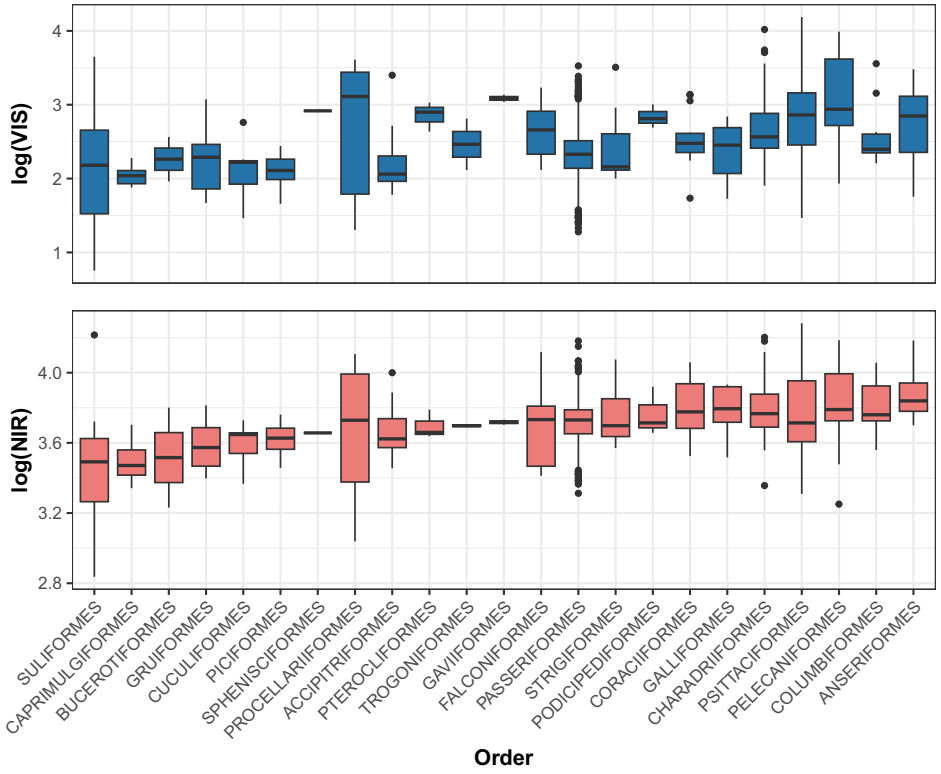

Figure 3. Variation in VIS and NIR reflectance across bird orders ($n \geq 2$).

Table 1. Order-level PGLS models relating NIR and VIS plumage reflectance of bird species. Each model summarizes the relationship between mean NIR (700–2500 nm) and VIS (300–700 nm) reflectance for bird orders with sample size ≥6. Both variables were log-transformed prior to analysis. Slope and intercept values represent the medians of the coefficients obtained by fitting the PGLS model to 1000 phylogenetic trees extracted from birdtree.org. The 95% CI columns report equal-tailed credible intervals (the 2.5th–97.5th percentiles across 1000 models), reflecting uncertainty due to phylogenetic topology. When the lower and upper limits are identical (e.g. 0.314–0.314), this indicates a point interval (i.e. negligible across-tree variation). RMSE values represent the median root mean square error of the fitted relationships across 1000 trees. 'All' refers to the all-species PGLS model, summarized in the same way (median across 1000 trees with the corresponding 95% confidence interval).

order	*N*	slope	95% CI	intercept	95% CI	RMSE
all	531	0.309	0.306–0.310	2.961	2.951–2.970	0.225–0.246
Accipitriformes	15	0.314	0.314–0.314	2.969	2.969–2.969	0.165–0.205
Anseriformes	14	0.157	0.155–0.157	3.437	3.432–3.437	0.129–0.185
Charadriiformes	49	0.341	0.338–0.345	2.875	2.865–2.885	0.194–0.251
Columbiformes	10	0.209	0.154–0.241	3.263	3.182–3.403	0.146–0.205
Coraciiformes	13	0.361	0.358–0.370	2.856	2.835–2.863	0.166–0.237
Cuculiformes	9	0.27	0.270–0.270	3.035	3.035–3.035	0.089–0.159
Falconiformes	9	0.354	0.354–0.354	2.777	2.777–2.777	0.172–0.344
Galliformes	11	0.389	0.379–0.396	2.886	2.871–2.905	0.134–0.262
Gruiformes	6	0.264	0.264–0.264	2.990	2.990–2.990	0.124–0.213
Passeriformes	305	0.294	0.289–0.297	3.032	3.023–3.043	0.163–0.189
Pelecaniformes	11	0.377	0.377–0.377	2.638	2.638–2.638	0.300–0.450
Piciformes	20	0.253	0.235–0.260	3.094	3.074–3.142	0.090–0.108
Procellariiformes	7	0.412	0.412–0.412	2.571	2.571–2.571	0.333–0.690
Psittaciformes	10	0.328	0.328–0.328	2.861	2.861–2.861	0.341–0.431
Strigiformes	13	0.281	0.281–0.281	3.073	3.073–3.097	0.107–0.163
Suliformes	10	0.332	0.332–0.332	2.748	2.748–2.748	0.353–0.568

(c) VIS-NIR equations

For all 531 species in the dataset, we fitted PGLS linear models relating NIR and VIS reflectance. Order-level PGLS regression equations ($p < 0.05$) were calculated for bird orders with sample size ≥6 (table 1.) Across all species, NIR and VIS reflectance values were strongly correlated ($R^2 = 0.667$; electronic supplementary material, figure S3), supporting the feasibility of predicting NIR reflectance from VIS spectra. However, the slope coefficients varied significantly among orders ($p < 0.01$), indicating lineage-specific differences in spectral properties. Notably, Procellariiformes was the only order with a slope exceeding 0.4, suggesting that in this group, NIR reflectance increases more steeply per unit increase in VIS reflectance compared to other bird orders, possibly reflecting unique structural or pigment-related adaptations.

(d) Between-order variation in NIR–VIS reflectance relationship

All bird orders exhibited significant positive correlations between VIS and NIR reflectance, with a global slope of 0.309. However, the slope of this relationship varied from 0.157 to 0.412 across bird orders, indicating taxon-specific spectral responses. There are differences in the trends of NIR reflectance with VIS across orders, as determined by testing the significance of the interaction terms in the fitted models. Procellariiformes showed the steepest slope, suggesting that species in this group exhibit a greater change in NIR reflectance per unit change in VIS reflectance. In contrast, Anseriformes had the shallowest slope, which was significantly lower than those of Procellariiformes, Charadriiformes, Pelecaniformes and Suliformes ($p < 0.05$). The largest difference was observed between Anseriformes and Procellariiformes, with the lower slope in Anseriformes indicating more conservative variation in NIR reflectance relative to VIS reflectance. (figure 4).

(e) Between-order differences in NIR reflectance residuals

To assess between-order differences in NIR reflectance while controlling for VIS reflectance, we extracted species' residuals from the PGLS model and compared their distributions across bird orders using a Kruskal–Wallis rank sum test. These residuals represent the deviation of each species' NIR reflectance from the value predicted by the overall relationship with VIS reflectance. We found significant differences among orders ($p < 0.001$).

Procellariiformes had the lowest residuals, although this difference was not statistically significant. Charadriiformes, Gruiformes and Pelecaniformes exhibited significantly lower residuals than some other orders ($p < 0.01$), indicating that species in these groups tend to have lower NIR reflectance than expected from their VIS reflectance. In other words, for the same plumage colour (VIS reflectance), these groups exhibit lower NIR reflectance than other birds. In contrast, Galliformes showed relatively higher residuals, suggesting comparatively enhanced NIR reflectance. Generally speaking, shorebirds and seabirds particularly reduced NIR reflectance relative to the overall avian trend (figure 5).

(f) Species traits influencing the NIR–VIS reflectance relationship

We employed a phylogenetic linear model incorporating complete trait data for 531 species to conduct repeated analyses on 1000 trees, identifying factors influencing NIR reflectance. Model selection was highly consistent across trees: the same predictor set was selected as the best-supported model in 999 of 1000 trees. The best model used VIS reflectance, HWI, precipitation, temperature, habitat type and migration type as predictors. There were no significant interactions between VIS reflectance and any of the additional covariates. The best model followed the form:

$$\log(NIR) = \alpha \cdot \log(VIS) + \beta \cdot HWI + \delta \cdot Precipitation + \varepsilon \cdot Temperature + \theta_{Migration} + \gamma_{Habitat} \quad (3.1)$$

Controlling for the association between NIR and VIS reflectance and for phylogenetic relatedness (Pagel's $\lambda = 0.66$ to 0.88), species with higher HWI exhibited significantly lower NIR reflectance ($t = -2.51$ to -1.92, $p = 0.01$ to 0.06). Climatic variables emerged as strong predictors: species inhabiting wetter environments had significantly lower NIR reflectance (precipitation: $t = -3.71$ to -3.21, $p < 0.001$), whereas those from hotter regions exhibited significantly higher NIR reflectance (temperature: t = 2.25–2.68, $p = 0.01$–0.03).

Migration strategy showed weaker yet consistent effects: resident species had lower NIR reflectance relative to baseline migrants ($t = -3.18$ to -2.82, $p < 0.01$), whereas partial migrants did not differ significantly ($t = -0.46$ to -0.05, $p = 0.64$–0.96). Habitat type was also associated with variation in NIR reflectance. Species inhabiting desert environments tended to exhibit relatively higher NIR reflectance relative to baseline coastal ($t = 0.02$–0.60, $p = 0.55$–0.96), whereas species from other habitat types showed significantly lower NIR reflectance (e.g. forest: $t = -4.66$ to -4.03, $p < 0.001$; grassland: $t = -4.27$ to -3.73, $p < 0.001$).

Together, these results indicate that both morphological and ecological factors shape the evolution of avian NIR reflectance. In particular, precipitation and habitat represent robust environmental correlates, while temperature, HWI and migratory behaviour contribute additional but weaker associations (figure 6).

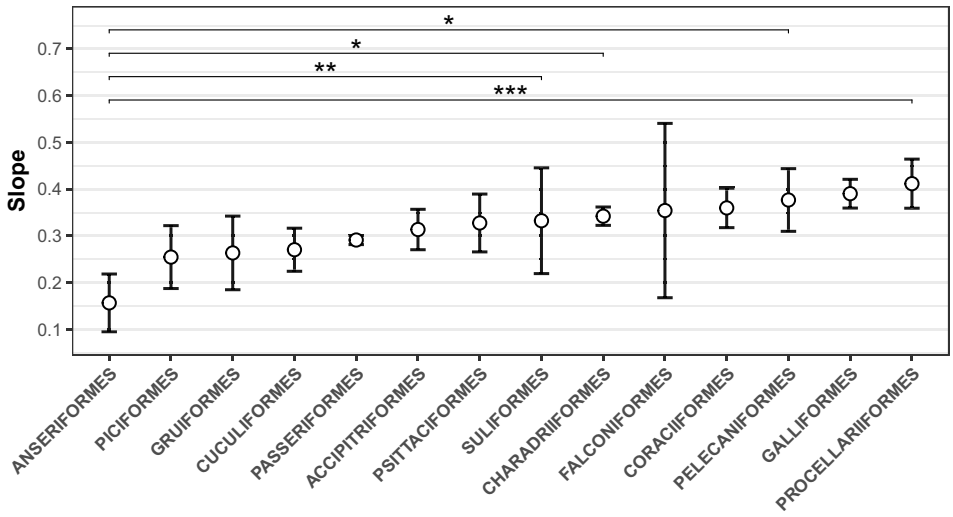

Figure 4. Variation in the relationship between NIR and VIS reflectance across bird orders. Slope estimates (± 95% CI) from order-specific linear models describing the relationship between NIR and VIS reflectance.

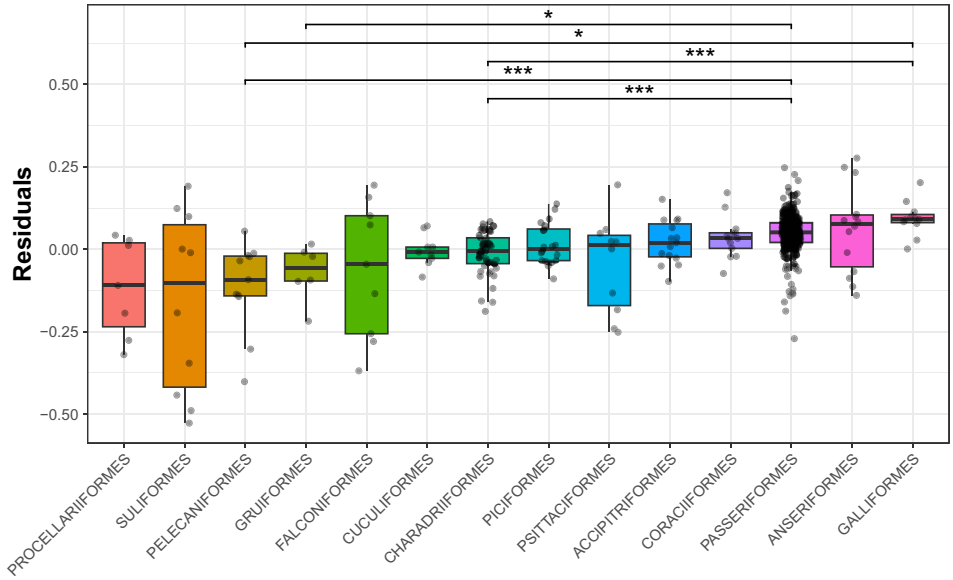

Figure 5. Between-order differences in residuals from the overall NIR–VIS reflectance PGLS model. Boxplots show the distribution of residuals grouped by avian order. Residuals reflect deviations in NIR reflectance relative to the global trend. A Kruskal–Wallis test revealed significant differences among orders ($p < 0.001$), with a moderate effect size ($\varepsilon^2 = 0.166$). Asterisks denote pairwise comparisons that remained significant after correction for multiple testing ($p < 0.05$).

4. Discussion

This study provides the first large-scale, taxonomically broad analysis of the relationship between NIR and VIS plumage reflectance for birds. By assembling a full-spectrum dataset for 531 species from 23 avian orders, we substantially expand the empirical basis for understanding avian plumage traits in the thermal infrared domain. Beyond establishing a strong overall correlation between VIS and NIR reflectance (R^2 = 0.667), we further developed order-specific regression models that allow NIR reflectance to be accurately predicted from VIS data. These models provide a practical tool for inferring NIR reflectance in species lacking direct measurements, thereby enhancing the utility of widely available VIS datasets in ecological and biophysical modelling.

By establishing a predictive framework for estimating NIR reflectance from VIS reflectance, our study expands the applicability of mechanistic niche models and biophysical simulations. Our findings are especially relevant for modelling thermal exposure, evaporative water loss, and habitat suitability under future climate change scenarios, particularly in regions subject to extreme heat or rapid land cover change [5,7,37]. Importantly, given that VIS reflectance data are far more readily available across museum collections and remote sensing platforms, our approach provides a scalable solution for estimating NIR properties in data-limited systems. This is particularly important for understudied taxa or historical specimens, and moreover helps to provide data support for correlations between NIR reflectance and the environment at the global scale [5]. In conservation contexts, the ability to infer NIR reflectance can enhance our capacity to assess species' vulnerability to thermal stress, particularly for wide-ranging migratory species and species inhabiting open habitats.

Previous studies have shown that structural coloration, which typically involves nanostructured keratin-air mats, and the major pigments that determine feather colour, such as melanin and carotenoids, modulate VIS reflectance [21,38,39]. In contrast, NIR reflectance appears more tightly linked to feather microstructure than to pigment content [12]. In related studies in other

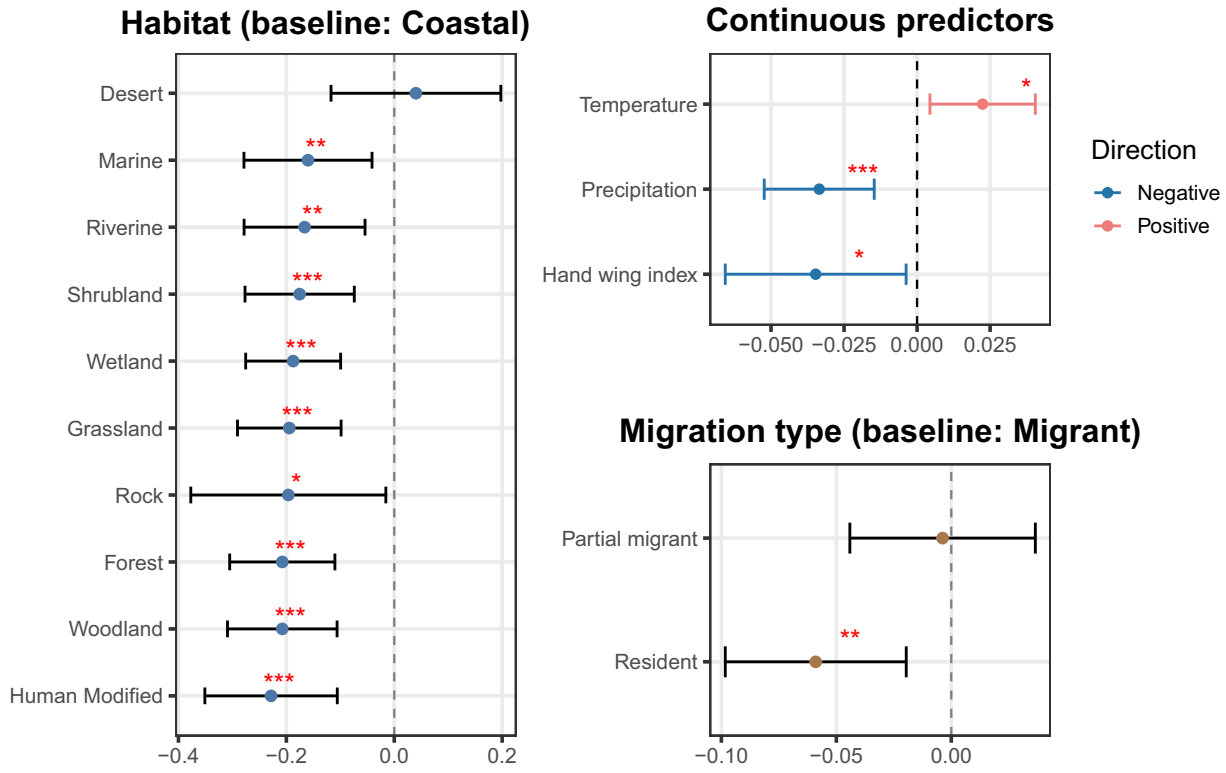

Figure 6. Effects of morphological and ecological traits on NIR reflectance. Each point represents effect sizes from the phylogenetic linear models. Error bars indicate 95% CI. The black dashed line marks the null effect (continuous predictors: slope = 0, habitat and migration type: intercept = 0). Asterisks denote statistically significant effects ($p < 0.05$).

disciplines, carotenoids do not have significant absorption peaks in NIR wavelengths, and absorption of melanin decreases steadily with increasing wavelength [40–42], suggesting that it is unlikely that they directly modulate feather NIR reflectance. However, avian eggshells with protoporphyrin pigments have very high NIR reflectance [10] because this pigments do not absorb NIR light, which is reflected by the calcium carbonate eggshell. Therefore, it is possible that species with specialized pigments, such as Psittaciformes, may have more complex determinants of NIR reflectance than other species due to the specific pigment absorption profiles and reflection properties of the feather structures. In summary, we assume that birds with different levels of colour richness may have different mechanisms for modulating NIR reflectance. In addition, the accumulation of airborne particulate matter on feathers also reduces reflectance, and there may be differences in reflectance of the same species in areas where airborne particulate matter varies [43].

In our study, despite the overall strong VIS–NIR correlation, we observed substantial variation in slope and residuals across bird orders. Order-specific regression models showed that the slope of the NIR–VIS relationship varied significantly across taxa, with Procellariiformes exhibiting particularly steep slopes. The residual analysis suggested that, for a given level of VIS reflectance, Charadriiformes and Pelecaniformes tend to have lower NIR reflectance than most other avian taxa. A similar, though not statistically significant, pattern was observed in Suliformes and Procellariiformes, potentially indicating the presence of specialized thermal regulation strategies in seabirds and shorebirds. In some shorebirds, such as members of the order Charadriiformes, thicker and shorter feather barbs are associated with enhanced feather hydrophobicity [44,45], and these morphological features may influence optical properties by modifying how incident radiation is intercepted, scattered, transmitted, or reflected within the feather layer. Differences in barb and barbule thickness, length, and density, together with feather posture (e.g. changes in feather depth due to ptiloerection), can alter the internal light-scattering environment and the penetration of NIR radiation, potentially contributing to lower and more variable NIR reflectance [10,12]. Seabirds are generally thought to be adapted to relatively cold marine environments because of their evolutionary origins [46,47], and their lower NIR reflectance is consistent with this pattern. However, our analyses are correlational, and we did not directly measure thermoregulatory performance, so it remains unclear whether lower NIR reflectance confers a thermal advantage or disadvantage. In the context of recent global warming, this plumage property may nevertheless be associated with greater thermal vulnerability in cold-adapted seabirds [48–50], but this interpretation should be tested directly in future work.

Our models show that migratory status may influence NIR reflectance. Studies have shown that migratory birds tend to have lighter plumage, which has been proposed to help reflect intense solar radiation encountered during long-distance flights, thereby reducing the risk of heat stress [11,24,51]. This is consistent with our finding that migratory species exhibit higher NIR reflectance compared to resident birds. Habitat type was also associated with variation in NIR reflectance. The relatively high NIR reflectance of desert taxa is broadly consistent with previous studies showing that species from hot, arid environments tend to exhibit elevated NIR reflectance, a trait that may reduce solar heat gain and associated water loss [5,7]. Coastal taxa also showed relatively high absolute NIR reflectance in our dataset. One possible explanation is that many coastal habitats are open and exposed, potentially increasing solar radiation load, although this interpretation remains tentative because we did not directly quantify microclimatic exposure or thermoregulatory consequences [47]. Importantly, this pattern does not

contradict our finding that shorebirds and seabirds tend to have negative residuals in the NIR–VIS relationship: while their absolute NIR reflectance is high, it is lower than expected given their VIS reflectance, indicating a relatively weaker increase in NIR reflectance for a given level of visible coloration. Considering the effect of feathers on flight efficiency, species with longer, more pointed wings often associated with long-distance flight, tend to have tighter feather structures [52,53], which may reduce NIR scattering and thereby modify reflectance properties. Such patterns suggest that habitat-specific thermal ecology and flight-related structural demands may drive variation in NIR reflectance in these taxa [53].

Climatic variables further explain substantial variation in reflectance. Species distributed in hot climatic zones exhibit higher NIR reflectance, potentially serving to reflect intense solar radiation [2,11]; whereas species inhabiting humid regions display lower NIR reflectance, probably due to weaker environmental radiation and more efficient evaporative cooling [22,39]. These findings indicate that both intrinsic traits and environmental pressures interact to shape the thermal and optical properties of avian plumage across ecological gradients. Analyses of model residuals further highlighted the ecological implications of between-clade NIR variations. Although shorebirds and seabirds may appear to have relatively high NIR reflectance in absolute terms, their steep slope indicates substantial variation in NIR–VIS scaling within the group. At the same time, their strongly negative residuals indicate that, for a given level of VIS reflectance, NIR reflectance is generally lower than expected. This pattern may represent adaptive flexibility for managing diverse thermal challenges across life stages and habitats, including breeding in open environments [54,55] and long migratory flights [56–58]. This contrasts with birds in hot, arid environments, where smaller species gain a greater advantage from high NIR reflectivity to minimize solar heat load [5,6,59]. For groups like Anseriformes and Galliformes, plumage coloration appears to be shaped more by camouflage and signalling functions than by thermoregulatory needs [60,61], suggesting that their elevated NIR reflectance may result from overlapping selection pressures related to both communication and thermal balance.

While our dataset is the most comprehensive of its kind to date, several limitations remain. First, despite broad taxonomic coverage, our dataset underrepresents tropical birds and taxa with highly variable or structurally complex coloration when compared to published databases of visible reflectance and body colouration. In addition, we did not consider differences in reflectance due to breeding plumage, and only analysed inter-taxon differences. Second, although linear models performed well across most groups, more complex relationships, such as the better fit of quadratic regression observed by Medina and colleagues in Australian birds [5], may require nonlinear or wavelength-specific approaches to fully capture reflectance variations due to feather microstructure or unique pigmentation, as well as adaptive differences shaped by different geographic distributions. Despite these limitations, our dataset provides a valuable resource for advancing understanding of avian thermoregulation. Future research could validate and refine these predictive models across a broader taxonomic and environmental spectrum, including intraspecific variation and ontogenetic changes. Integrating this framework with emerging technologies such as hyperspectral imaging and artificial intelligence may further enhance its resolution and ecological realism [62–64].

Ethics. This work did not require ethical approval from a human subject or animal welfare committee.

Data accessibility. All data associated with this manuscript are available at Dryad [65].

Supplementary material is available online [66].

Declaration of AI use. We have not used AI-assisted technologies in creating this article.

Authors' contributions. S.H.: data curation, formal analysis, funding acquisition, investigation, methodology, project administration, validation, visualization, writing—original draft, writing—review and editing; Y.D.: data curation, formal analysis, funding acquisition, investigation, methodology, project administration, visualization; Y.Z.: data curation, formal analysis, funding acquisition, investigation, methodology, project administration; D.S.-F.: methodology, supervision, writing—review and editing; Y.L.: resources, supervision, writing—review and editing; L.M.: conceptualization, funding acquisition, investigation, methodology, project administration, resources, supervision, writing—original draft, writing—review and editing.

All authors gave final approval for publication and agreed to be held accountable for the work performed therein.

Conflict of interest declaration. We declare we have no competing interests.

Funding. This study was supported by the National Natural Science Foundation of China (32570593, 32330067, 32501390) and the Fundamental Research Funds for the Central Universities, Sun Yat-sen University (24hytd014), and the Fundamental and Interdisciplinary Disciplines Breakthrough Plan of the Ministry of Education of China, and the University Student Innovation and Entrepreneurship Projects, Sun Yat-sen University (20241481).

Acknowledgements. We thank The Museum of Biology, Sun Yat-Sen University (SYSBM) and National Animal Collection Resource Center, Institute of Zoology, Chinese Academy of Sciences (NACRC, IOZCAS) for assistance and permission to use specimens. We also thank the collection manager, Peng He, for his support of the study, and the volunteers who participated in the reflectance measurements: Jingyi Liang, Tengtian Chen, Yuheng Zou and Zhen Pu. In addition, we thank Michael Kearney for his comments and support on the methodology and revision of the article. We thank Zhongwen Jiang for his suggestions on revising the article.

References

1. Maloney SK, Dawson TJ. 1995 The heat load from solar radiation on a large, diurnally active bird, the emu (*Dromaius novaehollandiae*). *J. Therm. Biol.* **20**, 381–387. (doi:10.1016/0306-4565(94)00073-R)
2. Wolf BO, Walsberg GE. 2000 The role of the plumage in heat transfer processes of birds. *Am. Zool.* **40**, 575–584. (doi:10.1093/icb/40.4.575)
3. Rogalla S, Shawkey MD, D'Alba L. 2022 Thermal effects of plumage coloration. *Ibis* **164**, 933–948. (doi:10.1111/ibi.13100)
4. McKechnie AE, Wolf BO. 2010 Climate change increases the likelihood of catastrophic avian mortality events during extreme heat waves. *Biol. Lett.* **6**, 253–256. (doi:10.1098/rsbl.2009.0702)
5. Medina I, Newton E, Kearney MR, Mulder RA, Porter WP, Stuart-Fox D. 2018 Reflection of near-infrared light confers thermal protection in birds. *Nat. Commun.* **9**, 3610. (doi:10.1038/s41467-018-05898-8)

6. Riddell EA, Iknayan KJ, Wolf BO, Sinervo B, Beissinger SR. 2019 Cooling requirements fueled the collapse of a desert bird community from climate change. *Proc. Natl Acad. Sci. USA* **116**, 21609–21615. (doi:10.1073/pnas.1908791116)
7. Ma L *et al*. 2023 Global patterns of climate change impacts on desert bird communities. *Nat. Commun.* **14**, 211. (doi:10.1038/s41467-023-35814-8)
8. Dale J, Dey CJ, Delhey K, Kempenaers B, Valcu M. 2015 The effects of life history and sexual selection on male and female plumage colouration. *Nature* **527**, 367–370. (doi:10.1038/nature15509)
9. Cooney CR, He Y, Varley ZK, Nouri LO, Moody CJA, Jardine MD, Liker A, Székely T, Thomas GH. 2022 Latitudinal gradients in avian colourfulness. *Nat. Ecol. Evol.* **6**, 622–629. (doi:10.1038/s41559-022-01714-1)
10. Stuart-Fox D, Newton E, Clusella-Trullas S. 2017 Thermal consequences of colour and near-infrared reflectance. *Phil. Trans. R. Soc. Lond. B* **372**, 20160345. (doi:10.1098/rstb.2016.0345)
11. Delhey K, Valcu M, Muck C, Dale J, Kempenaers B. 2023 Evolutionary predictors of the specific colors of birds. *Proc. Natl Acad. Sci. USA* **120**, e2217692120. (doi:10.1073/pnas.2217692120)
12. Stuart-Fox D, Newton E, Mulder RA, D'Alba L, Shawkey MD, Igic B. 2018 The microstructure of white feathers predicts their visible and near-infrared reflectance properties. *PLoS One* **13**, e0199129. (doi:10.1371/journal.pone.0199129)
13. Shawkey MD, Balenger SL, Hill GE, Johnson LS, Keyser AJ, Siefferman L. 2006 Mechanisms of evolutionary change in structural plumage coloration among bluebirds (*Sialia* spp.). *J. R. Soc. Interface* **3**, 527–532. (doi:10.1098/rsif.2006.0111)
14. Oud MD, Mahoney SM, Pageau C, de Menezes MA, Smith N, Briskie JV, Reudink MW. 2023 Global patterns of plumage color evolution in island-living passeriform birds. *PLoS One* **18**, e0294338. (doi:10.1371/journal.pone.0294338)
15. Porter CK, Romero FG, Adams DC, Bowie RCK, Riddell EA. 2023 Adaptive and non-adaptive convergent evolution in feather reflectance of California Channel Islands songbirds. *Proc. Biol. Sci.* **290**, 20231914. (doi:10.1098/rspb.2023.1914)
16. Conradie SR, Kearney MR, Wolf BO, Cunningham SJ, Freeman MT, Kemp R, McKechnie AE. 2023 An evaluation of a biophysical model for predicting avian thermoregulation in the heat. *J. Exp. Biol.* **226**, jeb245066. (doi:10.1242/jeb.245066)
17. Feldman A, Meiri S. 2013 Length-mass allometry in snakes. *Biol. J. Linn. Soc. Lond* **108**, 161–172. (doi:10.1111/j.1095-8312.2012.02001.x)
18. Feldman A, Sabath N, Pyron RA, Mayrose I, Meiri S. 2016 Body sizes and diversification rates of lizards, snakes, amphisbaenians and the tuatara. *Glob. Ecol. Biogeogr.* **25**, 187–197. (doi:10.1111/geb.12398)
19. Oskyrko O, Mi C, Meiri S, Du W. 2024 ReptTraits: a comprehensive dataset of ecological traits in reptiles. *Sci. Data* **11**, 243. (doi:10.1038/s41597-024-03079-5)
20. Luo DG, Yue WWS, Ala-Laurila P, Yau KW. 2011 Activation of visual pigments by light and heat. *Science* **332**, 1307–1312. (doi:10.1126/science.1200172)
21. Eliason CM, Shawkey MD, Clarke JA. 2016 Evolutionary shifts in the melanin-based color system of birds. *Evolution* **70**, 445–455. (doi:10.1111/evo.12855)
22. Wu S, Zhang K, Wang B, Que P, Yang B, Xu Y. 2024 Disentangling ecological drivers of interspecific achromatic plumage variation in birds. *Global Ecol. Biogeogr.* **33**, e13892. (doi:10.1111/geb.13892)
23. Claramunt S. 2021 Flight efficiency explains differences in natal dispersal distances in birds. *Ecology* **102**, e03442. (doi:10.1002/ecy.3442)
24. Delhey K, Dale J, Valcu M, Kempenaers B. 2021 Migratory birds are lighter coloured. *Curr. Biol.* **31**, R1511–R1512. (doi:10.1016/j.cub.2021.10.048)
25. National Animal Collection Resource Center, Institute of Zoology, Chinese Academy of Sciences. 2025. Dataset of feather morphology of some bird specimens in National Animal Collection Resource Center. CSTR:19715.10.2_AVES.Morphology.00007. See http://museum.ioz.ac.cn/topic_detail.aspx?id=73901.
26. National Animal Collection Resource Center, Institute of Zoology, Chinese Academy of Sciences. 2025. Dataset of visible and near-infrared reflectance of plumage of some bird specimens in National Animal Collection Resource Center. CSTR:19715.10.2_AVES.Color.00006. See http://museum.ioz.ac.cn/topic_detail.aspx?id=73900.
27. Ospina-Rozo L, Roberts A, Stuart-Fox D. 2022 A generalized approach to characterize optical properties of natural objects. *Biol. J. Linn. Soc.* **137**, 534–555. (doi:10.1093/biolinnean/blac064)
28. Li M, Wu Y, Wu Y, Zhao D. 2017 Experimental and theoretical investigation on radiation loss for a fault arc between different material electrodes in an enclosed air tank. *J. Phys. D: Appl. Phys.* **50**, 485205. (doi:10.1088/1361-6463/aa90f8)
29. Rogalla S, Patil A, Dhinojwala A, Shawkey MD, D'Alba L. 2021 Enhanced photothermal absorption in iridescent feathers. *J. R. Soc. Interface* **18**, 20210252. (doi:10.1098/rsif.2021.0252)
30. Jetz W, Thomas GH, Joy JB, Hartmann K, Mooers AO. 2012 The global diversity of birds in space and time. *Nature* **491**, 444–448. (doi:10.1038/nature11631)
31. Yu G. 2020 Using ggtree to visualize data on tree-like structures. *Curr. Protoc. Bioinformatics* **69**, e96. (doi:10.1002/cpbi.96)
32. Schliep KP. 2011 phangorn: phylogenetic analysis in R. *Bioinformatics* **27**, 592–593. (doi:10.1093/bioinformatics/btq706)
33. Pek J, Wong O, Wong ACM. 2018 How to address non-normality: a taxonomy of approaches, reviewed, and illustrated. *Front Psychol* **9**, 2104. (doi:10.3389/fpsyg.2018.02104)
34. Tobias JA *et al*. 2022 AVONET: morphological, ecological and geographical data for all birds. *Ecol. Lett.* **25**, 581–597. (doi:10.1111/ele.13898)
35. Wagenmakers EJ, Farrell S. 2004 AIC model selection using Akaike weights. *Psychon. Bull. Rev.* **11**, 192–196. (doi:10.3758/bf03206482)
36. R Core Team. 2025 *R: a language and environment for statistical computing*. Vienna, Austria: R Foundation for Statistical Computing.
37. Strubbe D, Jiménez L, Barbosa AM, Davis AJS, Lens L, Rahbek C. 2023 Mechanistic models project bird invasions with accuracy. *Nat. Commun.* **14**, 2520. (doi:10.1038/s41467-023-38329-4)
38. Dufresne ER, Noh H, Saranathan V, Mochrie SGJ, Cao H, Prum RO. 2009 Self-assembly of amorphous biophotonic nanostructures by phase separation. *Soft Matter* **5**, 1792–1795. (doi:10.1039/b902775k)
39. Lukhele SM, Jones SEI, Seal Faith NE, Grether GF, Kirschel ANG. 2025 Climate underpins continent-wide patterns of carotenoid-based feather colour consistent with Gloger's observations. *J. Anim. Ecol.* **94**, 1046–1060. (doi:10.1111/1365-2656.70034)
40. Li W, Patil A, Zhou X, Wang Z, Xiao M, Shawkey MD, Gianneschi NC, Dhinojwala A. 2020 Characterization of broadband complex refractive index of synthetic melanin coatings and their changes after ultraviolet irradiation. *Appl. Phys. Lett.* **117**, 203701. (doi:10.1063/5.0024229)
41. Roy S, Wu J, Cao J, Disu J, Bharadwaj S, Meinert-Spyker E, Grover P, Kainerstorfer JM, Wood S. 2024 Exploring the impact and influence of melanin on frequency-domain near-infrared spectroscopy measurements. *J. Biomed. Opt.* **29**, S33310. (doi:10.1117/1.JBO.29.S3.S33310)
42. Lacerenza M *et al*. 2025 Challenging the skin pigmentation bias in tissue oximetry via time-domain near-infrared spectroscopy. *Biomed. Opt. Express* **16**, 690–708. (doi:10.1364/BOE.541239)
43. Ellis JL, Ponette-González AG, Fry M, Johnson JA. 2023 Reduced reflectance and altered color: the potential cost of external particulate matter accumulation on urban Rock Pigeon (*Columba livia*) feathers. *Front. Ecol. Evol.* **11**, 946624. (doi:10.3389/fevo.2023.946624)

44. McNaught MK, Owens IPF. 2002 Interspecific variation in plumage colour among birds: species recognition or light environment? *J. Evol. Biol.* **15**, 505–514. (doi:10.1046/j.1420-9101.2002.00431.x)
45. Rijke AM. 2018 Feather structure and behavioral patterns in seabirds. In *Seabirds* (ed. H Mikkola), pp. 8–20. London, UK: IntechOpen. (doi:10.5772/intechopen.77729)
46. Choy ES, O'Connor RS, Gilchrist HG, Hargreaves AL, Love OP, Vézina F, Elliott KH. 2021 Limited heat tolerance in a cold-adapted seabird: implications of a warming Arctic. *J. Exp. Biol.* **224**, jeb242168. (doi:10.1242/jeb.242168)
47. Cook TR *et al*. 2020 Parenting in a warming world: thermoregulatory responses to heat stress in an endangered seabird. *Conserv. Physiol.* **8**, coz109. (doi:10.1093/conphys/coz109)
48. Richards C, Collins SM, Fisher K, Blackmore RJ, Fifield DA, Bates AE. 2024 Burrow nests fall below critical temperatures of threatened seabirds but offer thermal refuge during extreme cold events. *FACETS* **9**, 1–11. (doi:10.1139/facets-2023-0131)
49. Xiong Y, Fan L, Chang Y, Xiao H, Lei F. 2024 Warm temperature is associated with reduced body mass and diversification rates while increasing extinction risks in cold-adapted seabirds. *Glob. Chang. Biol.* **30**, e70000. (doi:10.1111/gcb.70000)
50. Pecuchet L *et al*. 2025 Arctic and Subarctic marine heatwaves and their ecological impacts. *Front. Environ. Sci.* **13**, 1473890. (doi:10.3389/fenvs.2025.1473890)
51. Sjöberg S *et al*. 2021 Extreme altitudes during diurnal flights in a nocturnal songbird migrant. *Science* **372**, 646–648. (doi:10.1126/science.abe7291)
52. Bachmann T, Klän S, Baumgartner W, Klaas M, Schröder W, Wagner H. 2007 Morphometric characterisation of wing feathers of the barn owl *Tyto alba pratincola* and the pigeon *Columba livia*. *Front. Zool.* **4**, 23. (doi:10.1186/1742-9994-4-23)
53. Videler JJ. 2006 Feathers for flight. In *Avian flight*, pp. 48–67. Oxford, UK: Oxford University Press. (doi:10.1093/acprof:oso/9780199299928.003.0003)
54. Ryeland J, Weston MA, Symonds MRE. 2021 The importance of wetland margin microhabitat mosaics; the case of shorebirds and thermoregulation. *J. Appl. Ecol.* **58**, 382–391. (doi:10.1111/1365-2664.13769)
55. Gutiérrez JS, Catry T, Espinosa-Colín M, Masero JA, Granadeiro JP. 2023 Heat stress increases risk taking in foraging shorebirds. *Funct. Ecol.* **37**, 1005–1019. (doi:10.1111/1365-2435.14288)
56. Lindström Å, Klaassen M. 2003 High basal metabolic rates of shorebirds while in the Arctic: a circumpolar view. *Condor* **105**, 420–427. (doi:10.1093/condor/105.3.420)
57. Vaillancourt E, Prud'homme S, Haman F, Guglielmo CG, Weber JM. 2005 Energetics of a long-distance migrant shorebird (*Philomachus pugnax*) during cold exposure and running. *J. Exp. Biol.* **208**, 317–325. (doi:10.1242/jeb.01397)
58. Ruthrauff DR, Dekinga A, Gill RE, Summers RW, Piersma T. 2013 Ecological correlates of variable organ sizes and fat loads in the most northerly wintering shorebirds. *Can. J. Zool.* **91**, 698–705. (doi:10.1139/cjz-2013-0070)
59. Schoenjahn J, Pavey CR, Walter GH. 2021 A true desert falcon with a delayed onset of heat dissipation behaviour. *J. Arid Environ.* **190**, 104530. (doi:10.1016/j.jaridenv.2021.104530)
60. Gluckman TL, Cardoso GC. 2010 The dual function of barred plumage in birds: camouflage and communication. *J. Evol. Biol.* **23**, 2501–2506. (doi:10.1111/j.1420-9101.2010.02109.x)
61. Marshall KLA, Gluckman TL. 2015 The evolution of pattern camouflage strategies in waterfowl and game birds. *Ecol. Evol.* **5**, 1981–1991. (doi:10.1002/ece3.1482)
62. Hogan BG, Stoddard MC. 2024 Hyperspectral imaging in animal coloration research: a user-friendly pipeline for image generation, analysis, and integration with 3D modeling. *PLoS Biol.* **22**, e3002867. (doi:10.1371/journal.pbio.3002867)
63. Levy O, Shahar S. 2024 Artificial intelligence for climate change biology: from data collection to predictions. *Integr. Comp. Biol.* **64**, 953–974. (doi:10.1093/icb/icae127)
64. Strydom LH, Conradie SR, Smit IPJ, Greve M, Boucher PB, Davies AB, McKechnie AE. 2025 Mapping tree canopy thermal refugia for birds using biophysical models and LiDAR. *Int. J. Biometeorol.* **69**, 2461–2474. (doi:10.1007/s00484-024-02833-z)
65. He S, Deng Y, Zhang Y, Stuart-Fox D, Ma L, Liu Y. 2025 Data from: From colour to heat: linking visible and near-infrared reflectance in birds. *Dryad Digital Repository.* (doi:10.5061/dryad.v15dv429d)
66. He S, Deng Y, Zhang Y, Stuart-Fox D, Liu Y, Ma L. 2026 Supplementary material from: From colour to heat: linking visible and near-infrared reflectance in birds. Figshare. (doi:10.6084/m9.figshare.c.8536173)